

remove ethyl alcohol. Furthermore, the lyophilized powder was stored in a moisture-proof container until needed. The morphology of quercetin nanoparticles was observed using a 20 kV SEM (Quanta 3D FEG/FEI).

The QNPs were initially analyzed by using FTIR to identify functional groups, phytochemical constituents, and other factors involved in the reduction and stabilization of the synthesized nanoparticles by using the Jasco FTIR 4100's attenuated total reflectance mode (Japan). The data was recorded between 4000 cm^{-1} and 400 cm^{-1} . CuK1-X Ray diffractometer radiation ($= 1.5406 \text{ \AA}$) was used to confirm the presence of ZnO in the powdered sample as well as to analyze the crystallite structure and size. An NMR spectrometer (BRUKER) was used to measure the ^1H NMR 400MHz spectra using DMSO.

2.3. Cell Lines:

The cell lines used in the study were obtained from the ATCC, U.S.A. and maintained in cell culture as per ATCC guidelines. For long-term usage, the cell lines were cryopreserved in liquid N₂ containers. A total of two cell lines, Human Tumor Cell Line (Huh-7) (ATCC, U.S.A.) and Human Epithelial Amnion Cell Line (WISH) were used in the present study.

2.4. Antioxidant activity

The method outlined by Braca *et al.* was used to measure the free radical scavenging activity of quercetin and quercetin nanoparticles based on the scavenging activity of the stable 1,1-diphenyl-2-picrylhydrazyl (DPPH) free radical (Braca A *et al.*, 2002). Three milliliters of a 0.004% methanol solution of DPPH were mixed with various amounts of quercetin and QNPs. After 30 minutes, the absorbance at 517 nm was measured. To determine the percentage inhibitory activity, the formula $[(A_0 - A_1)/A_0] \times 100$ was used, where A₀ represents the absorbance of the control and A₁ represents the absorbance of the quercetin/QSRs or ascorbic acid (Standard). Inhibition curves were created in order to get IC₅₀ values.

2.5. Sub culturing of cell lines:

The monolayer culture was transferred to a second vessel by diluting the cells with trypsin. After the cell reached 80% confluency, the culture flask was removed from the CO₂ incubator. The old medium was completely removed from the flask and washed with 3ml of 1X PBS. Trypsin (3 ml, 0.25%) was added to that flask for 60 seconds and removed, leaving a few drops in the flask. The culture flasks were kept at 37⁰ C for 20 minutes until all the cells were released from the surface in the residual trypsin solution. Furthermore, the required amount of growth medium (10 ml) was added to suspend the cells with the help of a Pasteur pipette, and the cells were distributed equally in two flasks. Finally, the culture flasks were incubated at 37⁰C with 5% CO₂.

2.6. In-vitro cytotoxic activity using human cancer and normal cell lines using SRB assay:

SRB assays were used to test the in-vitro cytotoxic activity of quercetin and QNPs (Houghton PJ *et al.*, 1994]. In order for the 3x10³ cells per well to adhere to the 96-well microtiter plates, 150 μ l of fresh media were incubated with the cells for 24 hours. After 24 hours, quercetin and quercetin nanoparticles were added in triplicate along with

0, 12, 5, 25, 50, and 100 μ g/ml. The plates were subsequently incubated once more for 24 hours with quercetin and quercetin nanoparticles present. Cell growth was examined in the last stage (Vichai V & Kirtikara K. 2006). Immediately after the operation, the cells were fixed by adding 50 μ l of cool, 40% (w/v) trichloroacetic acid, and they were once more kept at 4 $^{\circ}$ C for an hour. The plates with wells were thoroughly cleaned with distilled water after the supernatant was removed from them. Following the procedure, the cells were fixed by adding 50 μ l of cool, 40% (w/v) trichloroacetic acid, and they were once more maintained for an hour at 4 $^{\circ}$ C. After removing the supernatant from the plates containing wells, they were thoroughly cleaned with distilled water. 50 μ l of SRB solution was added to each well after the plate had dried, and it was left to incubate for 30 min at room temperature. The unconnected SRB was eliminated by repeatedly washing the plate in 1% acetic acid. To solubilize the dye, 100 μ l of 10 mM Tris base was then added to each well. The plates were placed on a plate and gently shaken for 20 minutes. After that, the absorbance (OD) was measured at 570 nm using an ELISA reader. The formula below was used to compute the cell's survival percentage.

Percentage cell survival = O.D. (treated cells)/ O.D. (control cells).

2.7. In-vivo toxicity assay:

Thirty adult male albino rats were used in this study. The animals were divided into four groups: the control group (A), animals treated with diethylnitrosamine and acrylamide to induce oxidative stress and hepatocarcinoma (B, C, and D), and animals not treated. The group B mice were considered as positive controls. The rest of the C and D group mice were treated with the different concentrations of quercetin and QNPs via intraperitoneal injection, after the four weeks of diethylnitrosamine and acrylamide administration. The liver function test was performed after the treatment of quercetin and QNR.

Decapitation was used to sacrifice animals by cervical dislocation, and the cardiac puncture technique was used to collect five milliliters of blood in gel tubes. The blood samples were then centrifuged for 15 minutes at 3000rpm. Human Germany provided standard reagents for the Humalyser 3000, a semi-automatic chemistry analyzer. Before and after the experiment, blood (5 mL) was taken from the vein. Liver function tests were carried out by analysing the AST, ALP, and ALP enzymes (Exarchou V *et al.*, 2002).

2.8. Histopathological examination:

The liver tissues of the respective animals were fixed using 10% formaldehyde for 24 hours and embedded into paraffin after 16 h. Five to five m thick sections of each sample were obtained from the paraffin blocks. Each sample was stained using hematoxylin and eosin. The results were analyzed using a light microscope (Babu BH *et al.*, 2002).

2.9. Statistical analysis

SPSS v16 was used to analyze the results of our study, with all values expressed as a mean standard error of mean. For ANOVA, P values of 0.05 and 0.01 were measured as statistically significant.

3. Results and Discussion

3.1. Characterization of synthesized QNPs:

3.1.1. FTIR spectroscopic analysis:

Figure 2 displays the quercetin IR spectrum. The bands of absorption at 3325 cm⁻¹ correspond to the hydroxyl

group. The C-H bond peak can be found at 3060 cm⁻¹. Stretching of the aromatic C=C bond at 1604 cm⁻¹, where hydroxyl group intensity reduced following QNPS synthesis, indicates the presence of an aromatic nucleus. The findings made it abundantly evident that intermolecular hydrogen bonding took place in the QNPs. (Figure 3).

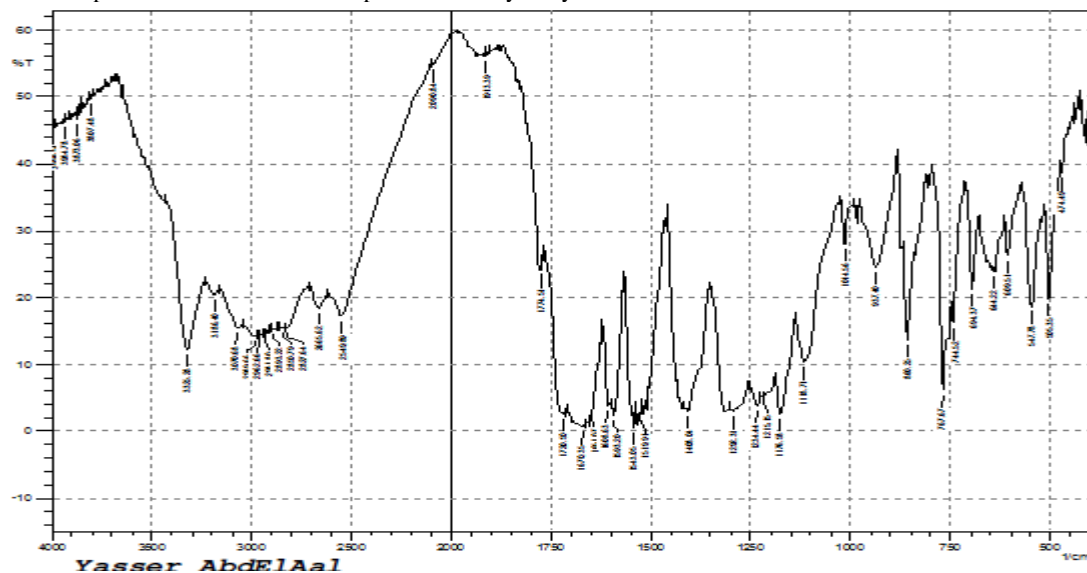


Figure2. IR spectrum of Quercetin

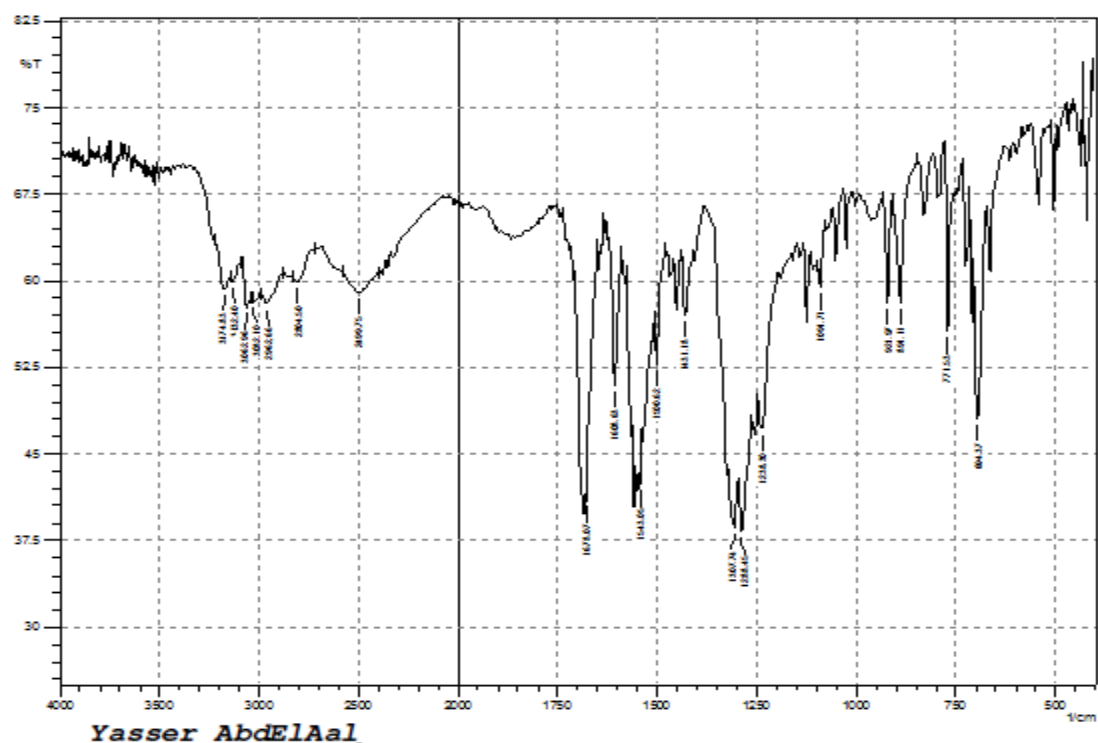


Figure3. IR spectrum of Quercetin nanoparticles

3.1.2. ¹H NMR spectrum of Quercetin and Quercetin nanoparticles:

The following values are displayed in the ¹H-NMR spectra of quercetin in DMSO-d₆ at 400 MHz: 11.24 (1H, s, C7-OH), 11.56 (1H, s, C4'-OH); 7.92 (1H, d, H-6), 7.94 (1H, d, H-8), 7.98 (1H, d, H-5'), 9.57 (1H, d, H-6'), and 9.87 (1H, s, H-2'). Furthermore, the aromatic proton had

peaks in the ¹H-NMR spectrum at C-6, C-8, C-5, C-6, and C-2, respectively (Figure 4). The spectra showed protons on aromatic groups ranging from 6 to 8 ppm, strong intramolecular hydrogen bonding at 12.62 ppm, a characteristic shift for intramolecular six-membered ring hydrogen bonding of the C5-OH and C4 O moiety. The QNP's results showed that the H6 and H8 aromatic protons had shifted upfield (Figure 5).

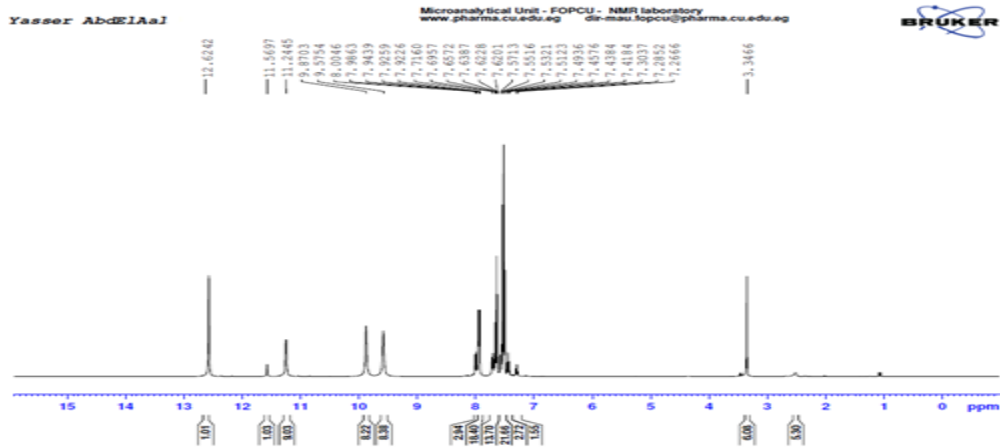


Figure4. ¹H NMR spectrum of Quercetin

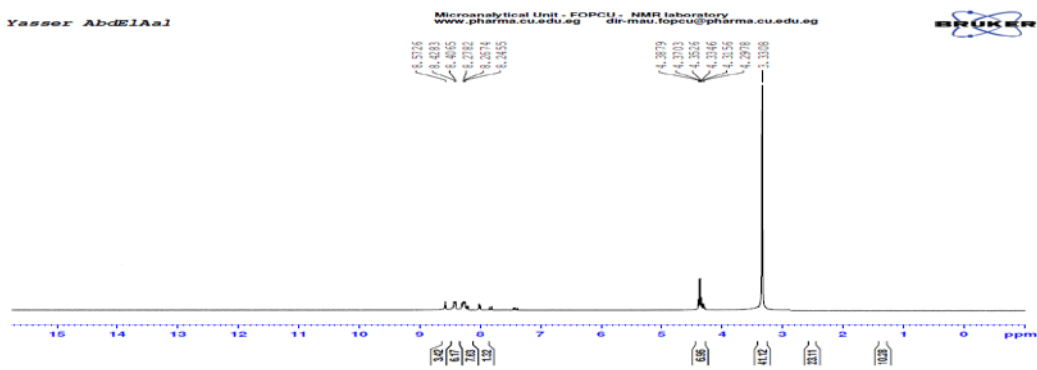


Figure5. ¹H NMR spectrum of Quercetin nanoparticles

3.1.3. XRD analysis:

By using X-ray diffraction, the dried crystalline quercetin nanoparticles were evaluated. The Quercetin nanocrystals' X-ray diffraction patterns are displayed in

Figure 6. Numerous distinct peaks of 12.61°, 14.5168°, 16.09°, 17.1714°, 18.62°, 20.19°, 21.17°, 23.78°, 26.10°, 27.91°, and 29.1808° were visible in the X-ray patterns of the QNPs (Figure 6).

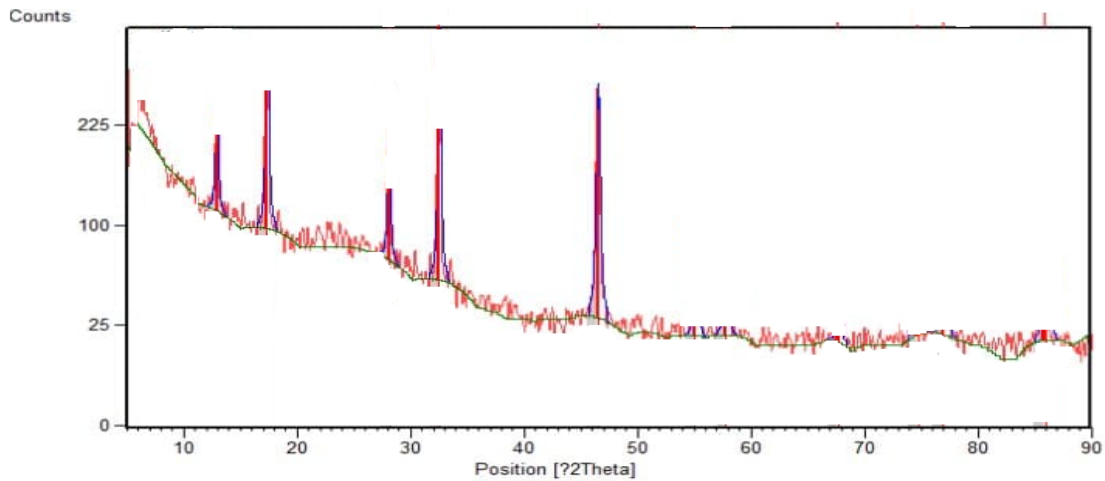


Figure6. X-ray diffraction of Quercetin nanoparticl

3.1.4. SEM analysis:

The size and crystalline properties of the produced NPs were studied by SEM examination. The QNPs' particle diameter was 17.25 nm at a flow rate of 8 ml/min. (Figure7).

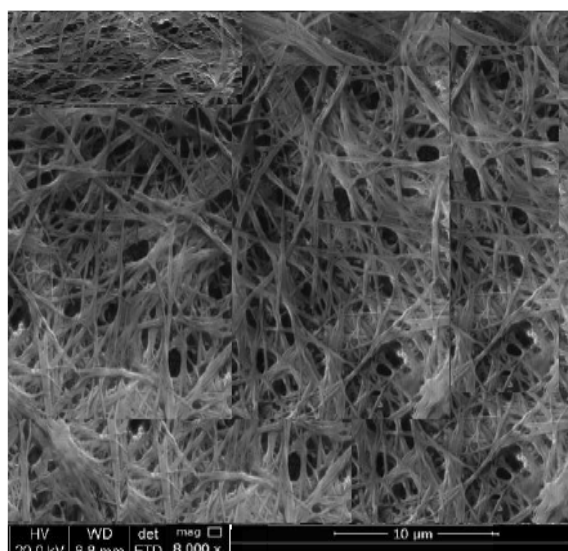


Figure 7. SEM photographs of Quercetin nanoparticles at flow rate (8ml/ min)

3.2. Biological activities:

3.2.1. Antioxidant activity:

A Quantitative analysis of quercetin and quercetin nanoparticles using the DPPH radical-scavenging method was then performed. Antioxidant activity using DPPH increased in a focus-dependent manner. In comparison to Ascorbic acid, Quercetin nanoparticles had a lower IC₅₀ value of 19.21 micrograms/ml (Table 1).

Table 1. Antioxidant activity of Quercetin and Quercetin nanoparticles, using DPPH free radical scavenging method

| Conc.(μg/ml) | Quercetin | Quercetin nanoparticles | Ascorbic Acid |
|------------------|--------------|-------------------------|---------------|
| 20 | 25.3 ± 0.23 | 45.12 ± 1.21 | 42.12 ± 0.22 |
| 40 | 27.11 ± 1.12 | 56.11 ± 0.21 | 47.13 ± 1.10 |
| 60 | 33.54 ± 2.12 | 62.3 ± 0.13 | 50.4 ± 1.11 |
| 80 | 35.7 ± 1.11 | 64.1 ± 1.53 | 55.1 ± 0.03 |
| 100 | 40.31 ± 0.19 | 69.32 ± 2.44 | 56.312 ± 0.11 |
| IC ₅₀ | 55.05 | 19.21 | 31.16 |

3.3. Cytotoxic activity:

3.3.1. In-Vitro cytotoxicity assay:

Human hepatocellular liver carcinoma (Huh-7) and a normal liver cell (WISH) were used to test the cytotoxicity of quercetin and quercetin nanoparticles. For each cell line,

IC₅₀ value was used to determine the toxicity. On the whole, quercetin nanoparticles were cytotoxic to human hepatocellular liver carcinoma (Huh-7, IC₅₀ 8.35 g/mL) but showed significantly less toxicity towards normal cells (Table 2).

Table 2. Percentage cell survival of Quercetin and Quercetin nanoparticles different cell lines

| Conc.(μg/ml) | Quercetin | Quercetin nanoparticles | WISH |
|------------------|-----------|-------------------------|-------|
| | Huh-7 | | |
| 0.0 | 2.000 | 1.068 | 1.160 |
| 12.5 | 1.868 | 0.600 | 1.891 |
| 25 | 1.659 | 0.415 | 1.531 |
| 50 | 1.222 | 0.325 | 1.375 |
| 100 | 1.232 | 0.222 | 1.291 |
| IC ₅₀ | 29.23 | 8.35 | 37.52 |

3.4. In-Vivo assay:

3.4.1. Biochemical analysis:

Earlier studies found that quercetin nanoparticles were highly effective against a liver cancer cell line (Huh-7). It was, therefore, decided to test the same cell line with quercetin nanoparticles *in-vivo*. The levels of AST (87.00 percent at 200 mg/kg.b.wt), ALT (50.00 percent at 200 mg/kg.b.wt), and albumin (317.11 at 200 mg/kg.b.wt) all showed dose-dependent anticancer activity (Table 3). The anticancer activity of quercetin nanoparticles (Figure 8) was confirmed by histopathology.

Table 3. In-vivo result of Quercetin and Quercetin nanoparticles

| Groups | Parameter | AST | ALT | ALP |
|--|-------------------|-------------|-------------|-------------|
| | Control group (A) | | 83.50±1.500 | 50.67±0.27 |
| Untreated group (B) | | 302.50±0.51 | 88.51±1.59 | 424.01±1.11 |
| Treated group (C) Quercetin | | 91.00±1.01 | 67.01±1.01 | 397.21±1.02 |
| Treated group (D) with Quercetin nanoparticles | | 87.00±1.21 | 50.00±1.05 | 317.11±1.11 |

(Mean±SD)

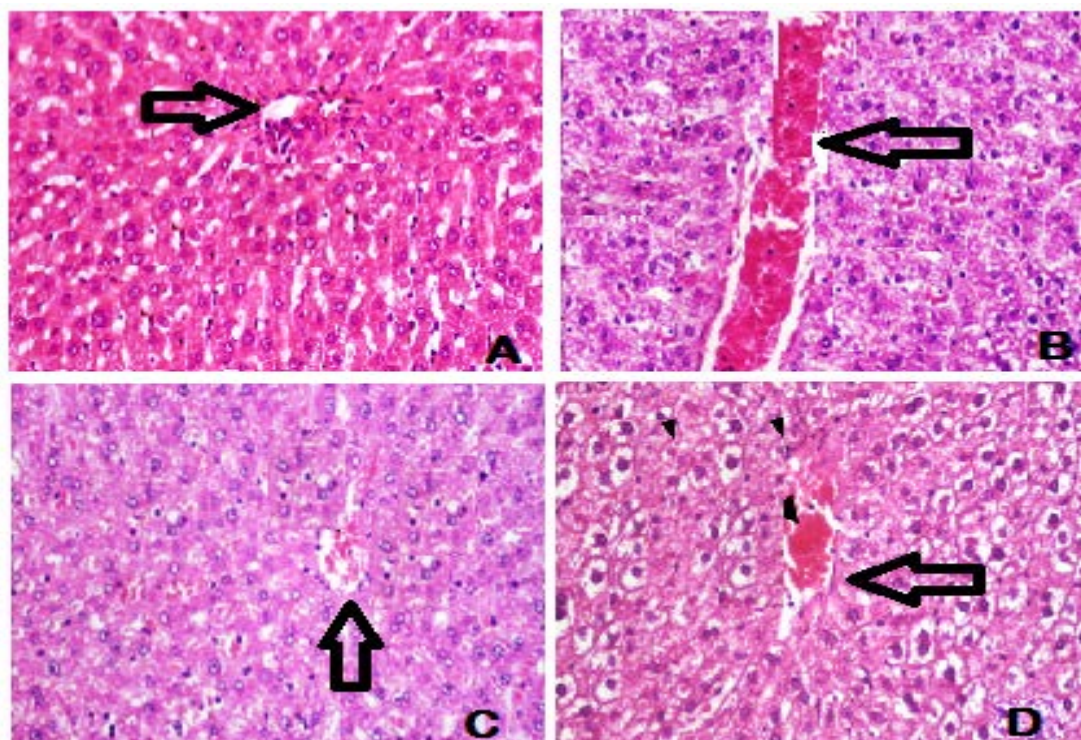


Figure 8: effect of Quercetin and Quercetin nanoparticles on livers section of different groups: **A)** of control rats revealed normal histological; **B)** induced control group (acrylamide) untreated with new compound; **C)** Experimental group treated with Quercetin and **D)** Experimental group treated with Quercetin nanoparticles.

3.5. Histopathological examination:

The hepatic lobules in the livers of rats in group 1 were found to be normal histologically (Figure 8A). Hepatocyte necrosis and fibroplasia were found in the portal triad in rats from group 2 (Figure 8B). Features include anaplastic carcinoma cells that are characterized by large hyperchromatic nuclei (Figure 8B). The quercetin treatment caused the acrylamide-induced rats to exhibit some nuclear pyknosis, granular and vacuolar degeneration, necrosis, and activation of Kupffer cells in the liver (Figure 8C).

Quercetin nanoparticle treated mice showed good restoration of the hepatic parenchymal cells with mild hepatocellular vacuolar degeneration and a few scattered necrotic cells (Figure 8D).

4. Conclusions

Quercetin is considered as one of the best naturally occurring flavonoids, consisting of several therapeutic properties, including anti-oxidative and anticancer (Butler MS. 2004) (Cho EJ *et al.*, 2003). Despite having several therapeutic properties, quercetin shows low bioavailability. According to Ren K *et al.*, (2017) QNPs displayed significant anticancer activity against, Hep3B, HCCLM3 and Bel7402MHCC97H (Ren K *et al.*, 2017). To overcome the problem of bioavailability and solubility, we also synthesized QNPs and then compared the *in-vitro* and *in-vivo* anticancer and antioxidative properties of quercetin and its nanoparticle QNP. The results indicated that the QNPs have an advantage over quercetin molecules as the QNPs showed better antioxidative and anticancer activity in *in-vitro* and *in-vivo* studies in comparison with quercetin molecules.

References

- Babu BH, Shylesh BS, Padikkala J. 2002. Tumour reducing and anticarcinogenic activity of *Acanthus ilicifolius* in mice. *J. Ethnopharmacol.*, **79**(1):27-33
- Bilati U, Allémann E, Doelker E. 2005. Development of a nanoprecipitation method intended for the entrapment of hydrophilic drugs into nanoparticles. *Eur J Pharm Sc.*, **24**(1):67-75
- Braca A, Sortino C, Politi M, Morelli I, Mendez J. 2002. Antioxidant activity of flavonoids from *Licania licaniaeflora*. *J. Ethnopharmacol.*, **79**(3):379-81.
- Butler MS. 2004. The role of natural product chemistry in drug discovery. *J. Nat. Prod.*, **67**(12):2141-53
- Cho EJ, Yokozawa T, Rhyu DY, Kim SC, Shibahara N, Park JC. 2003. Study on the inhibitory effects of Korean medicinal plants and their main compounds on the 1, 1-diphenyl-2-picrylhydrazyl radical. *Phytomedicine*. **10**(6-7):544-51.
- Dai J, Nagai T, Wang X, Zhang T, Meng M, Zhang Q. 2004. PH-sensitive nanoparticles for improving the oral bioavailability of cyclosporine A. *Int. J. Pharm.*, **280**(1-2):229-40.
- Exarchou V, Nenadis N, Tsimidou M, Gerothanassis IP, Troganis A, Boskou D. 2002. Antioxidant activities and phenolic composition of extracts from Greek oregano, Greek sage, and summer savory. *J. Agric. Food Chem.*, **50**(19):5294-9.
- Frenzel M, Steffen-Heins A. 2015. Impact of quercetin and fish oil encapsulation on bilayer membrane and oxidation stability of liposomes. *Food Chem.*, **185**:48-57.
- Houghton PJ, Photiou A, Uddin S, Shah P, Browning M, Jackson SJ, Retsas S. 1994. Activity of extracts of *Kigelia pinnata* against melanoma and renal carcinoma cell lines. *Planta med.*, **60**(05):430-3.

- Hsu CH, Cui Z, Mumper RJ, Jay M. 2003. Preparation and characterization of novel coenzyme Q10 nanoparticles engineered from microemulsion precursors. *AAPS Pharm SciTech.*, **4(3)**:24-35.
- Inal ME, Kahraman A. 2000. The protective effect of flavonol quercetin against ultraviolet a induced oxidative stress in rats. *Toxicology.*, **154(1-3)**:21-9
- Kanadaswami C, Lee LT, Lee PP, Hwang JJ, Ke FC, Huang YT, Lee MT. 2005. The antitumor activities of flavonoids. In-vivo., **19(5)**:895-909.
- Lee ES, Lee HE, Shin JY, Yoon S, Moon JO. 2003. The flavonoid quercetin inhibits dimethylnitrosamine-induced liver damage in rats. *J Pharm Pharmacol.*, **55(8)**:1169-74.
- Manna K, Debnath B, Das M, Marwein S. 2016. A comprehensive review on pharmacognostical investigation and pharmacology of *Typhonium trilobatum*. *J. Nat. Prod.*, **6(3)**:172-8.
- Omoriegbe ES, Oikeh EI. 2015. Comparative studies on the phytochemical composition, phenolic content and antioxidant activities of methanol leaf extracts of *Spondias mombin* and *Polyalthia longifolia*. *Jordan J. Biol. Sci.*, **147(3427)**:1-5.
- Prakash D, Gupta C, Sharma G. 2012. Importance of phytochemicals in nutraceuticals. *J. Chin. Med. Res.*, **1(3)**:70-8.
- Ren K, Li Y, Wu G, Ren J, Lu H, Li Z and Han X: 2017. Quercetin nanoparticles display antitumor activity via proliferation inhibition and apoptosis induction in liver cancer cells. *Int J Oncol.*, **50**: 1299-1311,
- Salatin S, Barar J, Barzegar-Jalali M, Adibkia K, Kiafar F, Jelvehgari M. 2017. Development of a nanoprecipitation method for the entrapment of a very water soluble drug into Eudragit RL nanoparticles. *Res Pharm Sci.*, **12(1)**:1
- Shikov AN, Tsitsilin AN, Pozharitskaya ON, Makarov VG, Heinrich M. 2017. Traditional and current food use of wild plants listed in the Russian Pharmacopoeia. *Frontiers in pharmacology.*, **8**:841
- Vichai V, Kirtikara K. 2006. Sulforhodamine B colorimetric assay for cytotoxicity screening. *Nature prot.*, **1(3)**:1112-6